

AN ABSTRACT OF THE THESIS OF

Robert Herman Hofeldt for the M.S. in Physical Chemistry
(Name) (Degree) (Major)

Date thesis is presented March 9, 1964

Title INTEGRATED INTENSITIES OF CARBON DIOXIDE
IN NUJOL SOLUTIONS

Abstract approved Redacted for Privacy
✓ (Major professor) ✓

The ratio of the absolute infrared intensity, A_3/A_2 , for the parallel mode (2336 cm^{-1}) and the perpendicular mode (658 cm^{-1}) of a nonpolar solute molecule, carbon dioxide, has been determined in a nonpolar solvent, Nujol. The solution ratio (5.0) which has been extrapolated to zero concentration is less than the corresponding gas phase ratio (11.2) as measured by other workers. Also a shift in the absorption peaks to lower frequencies has been observed. An attempt has been made to account for these differences between the solution and gas phase.

INTEGRATED INTENSITIES OF CARBON
DIOXIDE IN NUJOL SOLUTIONS

by

ROBERT T HERMAN HOFELDT

A THESIS

submitted to

OREGON STATE UNIVERSITY

in partial fulfillment of
the requirements for the
degree of

MASTER OF SCIENCE

June 1964

APPROVED:

Redacted for Privacy

Professor of Chemistry

In Charge of Major

Redacted for Privacy

Chairman of Department of Chemistry

Redacted for Privacy

Dean of Graduate School

Date thesis is presented March 9, 1964

Typed by Illa W. Atwood

ACKNOWLEDGMENT

I would like to express my most sincere gratitude to Professor J. C. Decius. I have been most fortunate to have been granted the privilege of doing this thesis and research under his guidance. His vast command of facts and his philosophical humor has been a most enlightening experience. Also, I take this opportunity to thank Dr. Raj K. Khanna for his many helpful comments and suggestions and whose friendship I shall always cherish.

Thanks are due to Mr. David M. Barnhart for his work on the computer, to Mrs. Atwood for her excellent job of typing, and to the many other professors and graduate students with whom I have become close friends.

TABLE OF CONTENTS

	Page
INTRODUCTION	1
THEORY AND DISCUSSION	3
Integrated Intensities	3
Absolute Intensities from Apparent Intensities	4
Dielectric Theory	9
Theory of Band Peak Shifts	13
Hot Bands	15
EXPERIMENTAL PROCEDURE	17
RESULTS AND CONCLUSIONS	23
BIBLIOGRAPHY	38
APPENDIX	40
Slit Function	40
Program Instructions for an Alvac IIIE, N = 64	40

LIST OF FIGURES

Figure		Page
1	Sample Flask	30
2	Vacuum Line	30
3	ν_2 mode	31
4	ν_3 mode	32
5	Plot of absorption area versus partial pressure of CO_2 for the ν_2 mode.	33
6	Plot of absorption area versus partial pressure of CO_2 for the ν_3 mode.	34
7	Plot of $K''B_2$ versus partial pressure of CO_2 for the ν_2 mode.	35
8	Plot of $K''B_3$ versus partial pressure of CO_2 for the ν_3 mode.	36
9	Plot of B_3/B_4 versus partial pressure of CO_2 .	37

LIST OF TABLES

Table		Page
I	Values of K for Various Values of $\ln(T_0/T)_{\nu_0}$ and $s/\Delta\nu_{\frac{1}{2}}^a$	26
II	Intensities	27
III	Solution to Gas Ratios	28
IV	Band Centers and Shifts	29

INTEGRATED INTENSITIES OF CARBON DIOXIDE IN NUJOL SOLUTIONS

INTRODUCTION

Carbon dioxide has been subjected to much intensive research. This stems from its abundance, its ease of preparation in nearly pure form, and to those in spectroscopy--its simple structure. Carbon dioxide is a linear, symmetrical triatomic molecule.

For any linear molecule with n atoms there are $3n-5$ modes of vibration. Of these $n-1$ are stretching vibrations, and $2n-4$ are bending vibrations. These modes of vibration are not always different. Due to symmetry factors, two or more vibrational modes may coincide, and if so, they are said to be degenerate; in the linear case under consideration, the $2n-4$ bending vibrations occur as $n-2$ doubly-degenerate pairs of modes.

Most molecules are in their lowest lying vibrational states. The spacings between these levels are of such magnitude that infrared radiation will excite transitions between the levels. For energy to be transferred between infrared radiation and the vibrating molecule, an electrical coupling must be present. This can occur only if the molecule produces an oscillating dipole moment that can interact with the electric field of radiation.

Carbon dioxide has four vibrational modes. Of these one is doubly degenerate; so there are only three distinct normal vibration frequencies. Since the symmetrical stretching mode has no oscillating dipole associated with its vibration, it is infrared inactive. The anti-symmetric stretching mode and the bending mode, which is doubly degenerate, are infrared active, for these do have an oscillating dipole associated with their vibrations.

From the infrared spectrum of the molecule absolute intensities may be determined which yield interesting and valuable information concerning the molecular environment (e.g., the effect of a surrounding dielectric medium upon a polarizable solute molecule) and the molecular properties (e.g., the electric dipole moment derivative).

THEORY AND DISCUSSION

Integrated Intensities

For monochromatic radiation of frequency ν (cm^{-1}) Beer-Lambert's law for an absorbing solute in a nonabsorbing solvent may be written

$$(I/I_0) = e^{-\alpha_\nu C \cdot L} \quad (1)$$

where I_0 and I are true incident and transmitted radiation intensities, respectively, C is the concentration of solute in moles per cc, and L is the cell length in centimeters.

If α_ν , the proportionality constant, is integrated over the entire band, one obtains the following result:

$$A = \int_{\text{band}} \alpha_\nu d\nu = \frac{1}{C \cdot L} \int_{\text{band}} \ln(I_0/I)_\nu d\nu \quad (2)$$

A , thus defined, is the true integrated absorption coefficient.

Since existing spectrophotometers have finite resolving powers, only intensities modified by the instrument are obtained. If T_0 and T are observed incident and transmitted intensities, respectively, and ν' is the observed frequency, the apparent integrated intensity, B , is given by

$$B = \frac{1}{C \cdot L} \int_{\text{band}} \ln(T_0/T)_{\nu'} d\nu' \quad (3)$$

Absolute Intensities from Apparent Intensities

Various methods have been advanced to transform apparent intensities into absolute or true intensities. Of these only a pertinent few will be mentioned and described.

E. B. Wilson, Jr. and A. J. Wells (21) in 1946 showed that if the incident intensity does not vary rapidly over the slit width and if the resolving power is high, as compared with the variation in α_{ν} , or similarly, if there is a constant resolving power over the band, then

$$\lim_{C \cdot L \rightarrow 0} B = A \quad (4)$$

Hence, true integrated intensities may be obtained from apparent intensities merely by plotting B versus $C \cdot L$ and extrapolating back to zero. However, this method suffers from the insensitive measurements at low concentrations or path lengths of B , C , and L , which are necessary for accurate extrapolation.

A slight improvement in the Wilson and Wells method was made by coworker, A. M. Thorndike, et al. (18). He found that B fluctuated considerably if calculated directly from experimental

data. So a quantity, **B**, is defined such that

$$\mathbf{B} = C \cdot L \cdot B \quad (5)$$

in which **B** is essentially the "absorption area." **B** is then plotted versus C, L, or C · L, and a smooth curve is fitted to the points.

The values of **B** obtained from this curve, i. e., the adjusted **B**'s, are used to determine the absolute intensity, A.

Assuming that the energy slit function can be represented by a triangular distribution and that the shape of an isolated band can be approximated by a Lorentz-type curve, D. A. Ramsay (17) in 1952 showed that

$$A = \frac{K}{C \cdot L} \cdot \ln(T_o / T)_{\nu_o} \Delta\nu_{\frac{1}{2}}^a \quad (6)$$

where $\Delta\nu_{\frac{1}{2}}^a$ is the apparent half band width,

$$K = \frac{\pi}{2} \cdot \frac{\ln(I_o / I)_{\nu_o}}{\ln(T_o / T)_{\nu'_o}} \frac{\Delta\nu_{\frac{1}{2}}^t}{\Delta\nu_{\frac{1}{2}}^a}$$

and $\Delta\nu_{\frac{1}{2}}^t$ is the true half band width. Table 1 reproduces Ramsay's values for K.

The Wilson and Wells procedure does not allow detection of concentration effects due to solute-solvent interaction; whereas, the Ramsay procedure assumes that the true band shape is Lorentzian

and that the slit function is triangular. A more flexible method which assumes only a spectrophotometer function (not necessarily triangular) has been devised by A. L. Khidir and J. C. Decius (9) in 1962.

These investigators have suggested that the true intensity, the observed intensity, and the spectrophotometer transformation may be represented by vectors \underline{i} and \underline{t} and a matrix, \underline{S} , respectively. The true intensity is transformed by the spectrophotometer into the observed intensity suggesting that

$$\underline{t} = \underline{S} \underline{i} \quad (8)$$

Using the identity

$$\underline{S}^{-1} \underline{S} = \underline{E} \quad (9)$$

where \underline{E} is the identity matrix and \underline{S} is a non-singular, cyclic matrix, one can show that

$$\underline{i} = \underline{S}^{-1} \underline{t} \quad (10)$$

The inverse matrix, \underline{S}^{-1} , may be computed from the unitary matrix, \underline{U} , and the diagonal matrix, \underline{D} , as follows:

$$\underline{S}^{-1} = \underline{U}^+ \underline{D}^{-1} \underline{U} \quad (11)$$

where \underline{U}^\dagger is the transpose conjugate. The elements of the matrix, \underline{D} , may be expressed as

$$\begin{aligned} D_{kk'} &= \delta_{kk'} D(k) \\ &= a_0 + \sum_j 2a_j \cos \frac{2\pi jk}{N} ; j = 1, \dots, N-1 \end{aligned} \quad (12)$$

where N is the number rows and columns in \underline{S} and the a 's are dependent upon the type of slit function chosen to represent the slit function. The elements for \underline{S}^{-1} are

$$S_{pq}^{-1} = \frac{1}{N} \left[1 + 2 \sum_{k=1}^{\frac{n-1}{2}} D^{-1}(k) \cos \frac{2\pi k(p-q)}{N} \right] \quad (13)$$

for N is odd, and

$$S_{pq}^{-1} = \frac{1}{N} \left[1 + 2 \sum_{k=1}^{\frac{N-2}{2}} D^{-1}(k) \cos \frac{2\pi k(p-q)}{N} + \frac{(-1)^{p-q} D^{-1} N}{2} \right] \quad (14)$$

for N is even.

Here one is confronted with a most disappointing result.

Since the elements of \underline{S}^{-1} are all large as compared to unity and

the calculated values of \underline{i} are linear combinations of all the t 's, the error in i_i is 10-15 percent for a 0.1 percent experimental error in T , i.e.

$$\underline{i} = (i_i) \quad (15)$$

and
$$\underline{S} = (S_{ij}) \quad (16)$$

then
$$i_i = \sum_k^N S_{ik} \cdot t_k \quad (17)$$

All is not lost, however, for a slightly different approach may be utilized. One may consider the difference

$$\underline{i} - \underline{t} = (\underline{E} - \underline{S}) \underline{i} \quad (18)$$

If $\underline{i} - \underline{t}$ is small and initially $\underline{i}_0 = \underline{t}$, the iterative process is given by

$$\underline{i}_n - \underline{t} = (\underline{E} - \underline{S}) \underline{i}_{n-1} \quad (19)$$

The aid of an automatic digital computer can be enlisted to mitigate the messy computations involved (see Appendix for further information).

Dielectric Theory

The early investigators were quick to recognize that the absolute intensities of the gas and liquid (or solution phase) did not yield the same values. Neither time nor effort was spared to solve this vexing riddle. S. R. Polo and M. K. Wilson (16) in 1955 applied the theory of dielectric polarization but made no distinction between polar and non-polar molecules. Their results for the liquid to gas phase intensity ratio is

$$A_L / A_g = \frac{1}{n} \left[\frac{n^2 + 2}{3} \right]^2 \quad (20)$$

where n is the refractive index of the dielectric medium. An extension to solution phase was made by W. B. Person (15) in 1958, where

$$\frac{A_{\text{soln}}}{A_{\text{gas}}} = \frac{1}{n} \left[\frac{n_o^2 + 2}{(n_o/n)^2 + 2} \right]^2 \quad (21)$$

and n_o and n are the refractive indices of the solute and solvent, respectively.

Extending A. D. Buckingham's quantum mechanical perturbation treatment (5) to a linear, symmetrical, triatomic molecule,

O. F. Kalman and J. C. Decius (8) obtained for the ν_3 mode

$$\frac{A_{\text{soln}}}{A_{\text{gas}}} = \frac{1}{3} \left[\frac{3n^2}{2n^2 + 1} \right]^2 \left[\frac{1}{1 - g\alpha_x} \right]^2 \quad (22)$$

where α_x , the polarizability along the x axis, is taken along the molecular axis of the molecule, n is the refractive index of the medium which for very dilute solutions can be taken to be that of the pure solvent, and g which is given by

$$\frac{2(n^2 - 1)}{2n^2 + 1} \cdot \frac{1}{r^3} \quad (23)$$

where r is the radius of the cavity. A similar expression for the α_2 mode may be obtained simply by replacing α_x with α_y , the polarizability along the Y or Z axis. Here, as elsewhere in this paper, the validity of Maxwell's relationship, $\epsilon = n^2$, has been assumed, where ϵ is the dielectric constant of the non-polar medium.

Until now the absorbing molecule has been considered to be centrally located within a spherical cavity surrounded by a continuous dielectric medium. Kalman and Decius (8) considered the case of an absorbing molecule possessing anisotropic polarization that

was centrally located within an ellipsoidal cavity. Their expression for the intensity ratio, $(A_{\text{soln}}/A_{\text{gas}})_i$, for the ν_i mode in the case of carbon dioxide is

$$\frac{A_{\text{soln}}}{A_{\text{gas}}}_i = \frac{1}{n} \left[\frac{n^2}{n^2 + (1 - n^2)A'} \right]^2 \left[\frac{1}{1 - g_i \alpha_i} \right]^2 \quad (24)$$

in which g_i , the reaction field factor, is equal to

$$\frac{3A'(1 - A')(n^2 - 1)}{a \cdot b \cdot c [n^2 + (1 - n^2)A']} \quad (25)$$

According to Böttcher (4, p. 72-74)

$$A' = \frac{a \cdot b \cdot c}{2} \int_0^\infty \frac{ds}{(s+a)^{2,3/2} (s+b)^{2,1/2} (s+c)^{2,1/2}} \quad (26)$$

where $2a$, $2b$, and $2c$ are the major and minor axis of the ellipsoidal cavity with a being taken in the direction of the induced dipole.

When a , b , and c are set equal to one another as in the case of a spherical cavity, elementary integration of equation (26) yields $A' = 1/3$. If this value for A' is substituted into equations (24) and (25), equations (22) and (23), respectively, are obtained as is reasonably expected. In the case of ν_3 mode the vibrating dipole

lies along the molecular axis of the carbon dioxide molecule, i. e.

a is the major axis, b is equal to c , and A' is equal to

$$\frac{a b^2}{2} \int_0^{\infty} \frac{ds}{(s+a^2)^{3/2} (s+b^2)} \quad (27)$$

Consulting appropriate tables for the integrals, equation (27)

is evaluated to be

$$A' = \frac{1}{2(P^2 - 1)} \left[\frac{P}{2\sqrt{P^2 - 1}} \ln \frac{P + \sqrt{P^2 - 1}}{P - \sqrt{P^2 - 1}} - 2 \right] \quad (28)$$

where $P = a/b = \alpha_x / \alpha_y$. For the ν_2 mode a must be chosen as the axis perpendicular to the molecular axis, a and c are equal to each other, and

$$A' = \frac{a^2 b}{2} \int_0^{\infty} \frac{ds}{(s+a^2)^2 (s+b^2)^{\frac{1}{2}}} \quad (29)$$

$$= \frac{P}{2(P^2 - 1)} \left[P - \frac{1}{2\sqrt{P^2 - 1}} \ln \frac{P + \sqrt{P^2 - 1}}{P - \sqrt{P^2 - 1}} \right] \quad (30)$$

where now $P = b/a = \alpha_x / \alpha_y$.

Theory of Band Peak Shifts

Increasing the pressure upon a gas, condensing a gas to liquid phase, or introducing a gas into solution phase have long been known to shift the band centers, often to lower frequencies, as compared to the low pressure gas phase band centers. An attempt will be made to account for this anomaly in the case of carbon dioxide in a non-polar solvent.

An expression relating the absolute intensity, A_i , to the change in the dipole moment with respect to the normal coordinates, i. e., $(\partial\mu/\partial Q)_{Q=0}$, is given here without derivation (1, p. 66-80; 17, p. 294-306; and 20, p. 162-166),

$$A_i = \frac{N\pi}{3 \cdot c^2} \left[\left(\frac{\partial\mu_x}{\partial Q_i} \right)_{Q=0}^2 + \left(\frac{\partial\mu_y}{\partial Q_i} \right)_{Q=0}^2 + \left(\frac{\partial\mu_z}{\partial Q_i} \right)_{Q=0}^2 \right] \quad (31)$$

where N is the number of molecules per cc, c is the velocity of light, and μ_x , μ_y , and μ_z are the X, Y, and Z components of the dipole moment. The derivative of the dipole moment is taken at the equilibrium position, $Q=0$.

The antisymmetric stretching mode for carbon dioxide has

$$\left(\frac{\partial\mu_y}{\partial Q_3} \right)_{Q=0} = \left(\frac{\partial\mu_z}{\partial Q_3} \right)_{Q=0} = 0; \text{ so}$$

$$A_3 = \frac{N\pi}{3 \cdot c^2} \left[\frac{\partial \mu_x}{\partial Q_3} \right]_{Q=0}^2 \quad (32)$$

The bending mode has $(\partial \mu_y / \partial Q_2)_{Q=0} = (\partial \mu_z / \partial Q_2)_{Q=0} \neq 0$ and

$(\partial \mu_x / \partial Q_2)_{Q=0} = 0$, hence

$$A_2 = \frac{2 \cdot N\pi}{3 \cdot c^2} \left[\frac{\partial \mu_y}{\partial Q_2} \right]_{Q=0}^2 \quad (33)$$

Using the Onsager model of dipole-induced dipole interaction (22), (10) and (12) of a solute molecule contained within a spherical cavity of radius r surrounded by homogeneous solvent of refractive index n , the frequency shift, $\Delta \nu_i$, is equal to

$$-\frac{g}{2} \left[\frac{\partial \mu_i}{\partial Q_i} \right]_{Q=0}^2 \quad \frac{1}{8\pi^2 c^2 \nu_i^0 d_i} \quad (34)$$

in which ν_i^0 is the gas phase frequency. For carbon dioxide in a non-polar solvent, the frequency shifts upon combination of equations (32), (33) and (34) becomes

$$-\frac{n^2 - 1}{2n^2 + 1} \frac{1}{r^3} \frac{3 \cdot A_i}{8\pi^3 \cdot N \cdot \nu_i^0 d_i} \quad (35)$$

where d_i is the degeneracy of the i^{th} mode.

If the reaction field term for a spherical cavity can be

replaced with the reaction field term for an ellipsoidal cavity, one obtains for the ν_i vibrational mode

$$\Delta \nu_i = - \frac{g_i}{2} \frac{3 \cdot A_i}{8\pi^3 N \cdot \nu_i^0 d_i} \quad (36)$$

where g_i is given by Equation (25).

Hot Bands

At room temperature most molecules are in their lowest lying vibrational states, i.e., if ν_i is the vibrational quantum number of the molecule, $\nu_i = 0$ for all values of i . However, should the spacing between the lowest and a next higher level be small as compared to kT , the Boltzmann distribution will allow sufficient number of molecules to reside in this excited state

The energy in wavenumbers, $\bar{\epsilon}(\nu_1, \nu_2, \dots, \nu_{3n-6})$, for a vibrational anharmonic oscillator with cross terms in the potential energy function is

$$\sum_i^{3n-6} \omega_i \left(\nu_i + \frac{1}{2} \right) + \sum_i^{3n-6} \sum_{j \geq i}^{3n-6} X_{ij} \left(\nu_i + \frac{1}{2} \right) \left(\nu_j + \frac{1}{2} \right) \quad (37)$$

in which ω_i is the classical vibrational frequency measured in

wavenumbers and X_{ij} is the anharmonicity constant.

In the case of carbon dioxide the antisymmetric stretching fundamental corresponds to a

$$v_3 = 0, \quad v_2 = 0, \quad v_1 = 0 \quad \rightarrow \quad v_3 = 1, \quad v_2 = 0, \quad v_1 = 0$$

transition, or more amply stated in mathematical terminology

$$\Delta \bar{\epsilon}_3 = \bar{\epsilon}(1, 0, 0) - \bar{\epsilon}(0, 0, 0) = \omega_3 - \frac{1}{2}X_{13} - \frac{1}{2}X_{23} - 2X_{33} \quad (38)$$

The energy for an excited transition, i. e., hot band, of the type

$$v_3 = 0, \quad v_2 = 1, \quad v_1 = 0 \quad \rightarrow \quad v_3 = 1, \quad v_2 = 1, \quad v_1 = 0$$

is

$$\Delta \bar{\epsilon}_{3_{\text{hot}}} = \bar{\epsilon}(1, 1, 0) - \bar{\epsilon}(0, 1, 0) = \omega_3 - \frac{1}{2}X_{13} - \frac{3}{2}X_{23} - 2X_{33} \quad (39)$$

The difference in energy for the two transitions is

$$\Delta \bar{\epsilon}_3 - \Delta \bar{\epsilon}_{3_{\text{hot}}} = -X_{23} \quad (40)$$

EXPERIMENTAL PROCEDURE

Nujol, a product of the Plough, Inc., functioned as the solvent throughout this experiment. It is a highly refined petroleum mineral oil free of any aromatic compounds. Selection for use as a solvent was based upon its availability, its non-polar properties, and its spectroscopic transparency in the regions of $630\text{-}700\text{ cm}^{-1}$ and $2180\text{-}2450\text{ cm}^{-1}$. Any dissolved gases were removed from the liquid by placing it under a vacuum of 10^{-1} centimeters of mercury or less. While it was in this state, heat was applied to facilitate the removal of the dissolved gases.

The carbon dioxide was obtained in the gaseous form from the Pure Carbonic Co. and in the solid form from the Liquid Carbonic Co. The gas obtained from cylinders was purified of water vapors by passing it through a drying tube containing anhydrous MgClO_4 . The carbon dioxide obtained from dry ice was purified by allowing it to sublime into a closed system initially at a pressure of 0.1 centimeter of mercury. The sublimation process and a dry-ice acetone cold trap (-80°C) removed any water vapor and high vapor pressure impurities. Scans from $600\text{-}4000\text{ cm}^{-1}$ were made of the two purified gases contained in ten centimeter gas cells. The amount of foreign absorbing gases was found to be negligible. All equipment was thoroughly cleaned, was dried in an oven maintained at

110° C, and was stored in a desiccator.

Tank CO₂ was passed through a 12 cc gas dispersion tube #39533 suspended in a 100 ml graduate cylinder containing Nujol. The CO₂ was bubbled through the gaseous-free Nujol at a fairly rapid rate for at least four hours. The solutions were saturated at 0° C and at partial pressures of CO₂ in excess of one atmosphere.

The saturated solution was placed in the container shown in Figure 1. The stopcock on the flask was closed, and the ball joint was greased with Apiezon M or N vacuum grease. The flask was then connected at 'b' (see Figure 2) to a previously evacuated vacuum line, and stopcock 'd' was opened (stopcock 'g' was closed and 'c' and 'p' were open). A Cenco HyVac vacuum pump #1232388 capable of obtaining a vacuum of about 10⁻² centimeters of mercury was connected to the vacuum line and was left pumping throughout the experiment.

A ball joint tube which had been previously sealed at one end was filled with crushed dry ice and was connected to the vacuum line at 'e', and at the same time 'g' was opened. When the pressure within the system was due to subliming CO₂ only, 'e' was submerged into a Dewar containing liquid nitrogen (-196° C). The system was pumped on for about a minute; then cold trap 'f' was chilled with a dry ice-acetone slush bath (-80° C). The Dewar was removed, and

'e' was allowed to warm to dry ice temperature (-78°C). From a change in the pitch of pumping sublimation of CO_2 was again assumed to be taking place. After several minutes of pumping 'c' was closed, and the gas was allowed to expand to a pressure pre-selected for equilibration. The pressure was quickly read, and the stopcock on the flask was opened. The pressure was again read; the difference was taken to be that due to air initially within the flask. The whole operation from the moment that the Nujol solution was placed into the flask until the stopcock on the flask was opened rarely took more than five minutes.

The CO_2 was left in contact with the Nujol solution for periods varying from four hours to three days. During equilibration the solution was maintained at $25.0 \pm 0.2^{\circ}\text{C}$ with a constant temperature bath. When equilibrium was thought to have been attained as verified by the reproducibility of results, the pressure as indicated by the mercury manometer connected at 'o' was recorded, 'a' was closed, and the flask was removed from the line.

A Perkin-Elmer fixed thickness cell #127-xx76 with NaCl windows was cleaned with reagent grade chloroform and was readied for use. A two milliliter hypodermic syringe with a four inch extension was employed to remove the equilibrated solution from the flask. The extension was fashioned from a discarded ball point

filler which had been soldered to the base of a hypodermic needle which had had a larger hole drilled out. Extreme caution was exercised while removing a sample from the flask to prevent suction of CO_2 from solution. The extension was removed, and solution was carefully injected into the fixed thickness cell. The orifices were sealed with Teflon plugs provided for this purpose.

The cell containing the solution was placed in the sample beam compartment of a Beckman IR-7 Spectrophotometer. The controls of the instrument were adjusted as specified in the instruction manual (3, p. 11-20). Double beam scans with air as reference were made from $630\text{-}700\text{ cm}^{-1}$ with a CsI Long Wavelength Interchange #49790 and from $2180\text{-}2450\text{ cm}^{-1}$ with a NaCl prism interchange. Similarly, unadulterated gaseous free Nujol was inserted into the cell, and double beam scans were made between the same two regions. The latter two scans were used as the base line (T_o values) for determining the absorption area, **B**.

The common logarithm of T_o/T was plotted versus the observed frequency, ν' . The resulting curve was traced three times with a planimeter, and the average was taken to be the absorption area.

Henry's law states that the partial pressures of component A, i. e., p_A , is proportional to its mole fraction, x_A , or

$$p_A = K_A \cdot x_A \quad (41)$$

where K_A is the Henry law constant. This was assumed to be valid for the dilute solutions of carbon dioxide in Nujol (about 10^{-5} mole/cm³). Also for dilute solutions x_A is proportional to C .

Hence, it can be shown that

$$B_i = \frac{2.303}{K''_p \cdot L} \int_{\text{band}} \log_{10} (T_o/T)_{\nu'_i} d\nu'_i \quad (42)$$

The empty cell was placed in the sample compartment of the IR-7 and was scanned double beam from 700 to 2000 cm⁻¹. From the number of fringes, n , within a given interval of frequencies, $\Delta \nu$, the cell length L was calculated using the formula

$$L = \frac{n}{2 \Delta \nu} \quad (43)$$

Figures 5 and 6 depict the plots of absorption area versus partial pressure of CO₂. Since neither the concentration nor K'' was obtained, the absolute intensity itself could not be determined. Figures 7 and 8 depict the plots of $B_i K''$ versus partial pressures of CO₂.

Gaseous carbon dioxide contained in ten centimeter gas cells

at pressures of 70 mm for the ν_2 band and about 50 mm for the ν_3 band was scanned for rotational structure. From the spectra and tabulated rotational values (7, p. 576 and 592) a correction of $+0.2 \text{ cm}^{-1}$ and -0.05 cm^{-1} were applied to the ν_2 and ν_3 band centers, respectively. The band centers for solution and gas are given in Table IV.

RESULTS AND CONCLUSIONS

To eliminate the unknown constant, K'' , the A_3 to A_2 ratio was computed for the solution. The same ratio was computed using the method of Ramsay. The method of Khidir and Decius was applied to the ν_2 mode. It was found that the increase in peak intensity was very nicely compensated by a decrease in band width (see Figure 3). Hence, the net effect was that the absorption area remains unchanged, i. e., any correction was well within the experimental error. Since the slit width to apparent half band width for the ν_3 band was considerably less than that for the ν_2 band, the apparent intensities were taken to be the true intensities, and the Khidir and Decius method was not applied. The gas phase intensities were those reported by Overend, et al. (13) for the perpendicular band and Weber, et al. (19) for the parallel band. The results are tabulated in Table II.

The polarizability of carbon dioxide calculated by Barrow (2, p. 298) are $\alpha_x = 4.10 \text{ \AA}^3$ and $\alpha_y = \alpha_z = 1.93 \text{ \AA}^3$. The radius of the cavity was taken to be equal to the van der Waals' diameter of CO_2 , 3.24 \AA . The volumes of the ellipsoidal and spherical cavities were assumed to be the same. For any given distillate fraction of petroleum the index of refraction is constant within 1-3 percent. The index of refraction for Nujol was taken to be the same as that

for mineral oil. Hence, for Nujol n is 1.478 (11, p. 310), and for CO_2 n_o is 1.000. Using the above data the A_{soln} to A_{gas} ratio were computed from equations (20), (21), (22), and (24). The results are tabulated in Table III.

If the absorption area, \mathbf{B} , for a given mode is plotted versus the partial pressure of carbon dioxide, Figures 5 and 6 are obtained. Figures 7 and 8 are produced when the values obtained from the smooth curves of 5 and 6 are multiplied by the factor $2.303/p \cdot L$, where $L = 0.0162$ cm and p is pressure in mm of mercury, then plotted against pressures. By plotting $\mathbf{B}_3/\mathbf{B}_2$ against pressure Figure 9 is obtained. The values of \mathbf{B}_i in these instances are taken from the smooth curve in 5 and 6. The results of 7 and 8 are tabulated in Table II.

Since the frequency shifts between solution and gas phases have been measured with a precision at least as good as the intensities, it is worthwhile to test the dielectric theory with these data. According to (35) and (36), one has

$$\frac{\Delta \nu_2}{\Delta \nu_3} = \frac{A_2 \nu_3^o}{2 A_3 \nu_2^o} \quad (44)$$

for the case of a spherical cavity, where g is obtained from (23), and

$$\frac{\Delta \nu_2}{\Delta \nu_3} = \frac{g_2 A_2 \nu_3^0}{2 g_3 A_3 \nu_2^0} \quad (45)$$

for an ellipsoidal cavity, where appropriate numerical values of g_2 and g_3 can be obtained from (25). Theoretical values of $\Delta \nu_2 / \Delta \nu_3$ for these models are given in Table IV.

A comparison of theoretical values of $(A_3/A_2)_{\text{soln}} : (A_3/A_2)_{\text{gas}}$ ratio in Table III to the experimental values in Table II indicate that the experimental value is smaller than that calculated for either the spherical or ellipsoidal cavity, although agreement is better in the latter case. However, the experimental ratio is still smaller, by nearly a factor of 1.5, so that in general the improved agreement with the ellipsoidal model obviously still does not represent a satisfactory theory of either intensity or frequency changes.

The constancy of the anharmonicity constant, X_{23} , seems to indicate that the difference between two vibrational frequencies having only one different vibrational quantum number remains unchanged upon emerging the gas molecule into the polarizable dielectric medium, i. e.,

$$\Delta \bar{\epsilon}(\nu_1, \nu_2, \dots, \nu_k, \dots, \nu_n) = \Delta \bar{\epsilon}(\nu_1, \nu_2, \dots, \nu_k', \dots, \nu_n)$$

is a constant where $\nu_k \neq \nu_k'$.

TABLE I

Values of K for Various Values of $\ln(T_o/T)_{v'_o}$ and $s/\Delta v_{\frac{1}{2}}^a$ (17)

$s/\Delta v_{\frac{1}{2}}^a$	$\ln(T_o/T)_{v'_o}$							
	2.0	1.8	1.6	1.4	1.2	1.0	0.8	0.6
0.00	1.57	1.57	1.57	1.57	1.57	1.57	1.57	1.57
0.05	1.57	1.57	1.57	1.57	1.57	1.57	1.57	1.57
0.10	1.57	1.57	1.57	1.57	1.57	1.57	1.57	1.56
0.15	1.57	1.57	1.57	1.57	1.57	1.56	1.56	1.56
0.20	1.57	1.57	1.57	1.57	1.56	1.56	1.56	1.55
0.25	1.57	1.57	1.57	1.56	1.56	1.55	1.55	1.55
0.30	1.57	1.57	1.57	1.56	1.56	1.55	1.54	1.54
0.35	1.57	1.57	1.57	1.56	1.55	1.54	1.53	1.53
0.40	1.58	1.57	1.57	1.56	1.55	1.54	1.52	1.51
0.45	1.59	1.58	1.57	1.56	1.54	1.53	1.51	1.50
0.50	1.60	1.58	1.57	1.56	1.54	1.52	1.50	1.48
0.55	1.62	1.60	1.58	1.56	1.54	1.52	1.49	1.46
0.60	1.65	1.62	1.59	1.56	1.54	1.51	1.48	1.45
0.65	1.68	1.64	1.60	1.56	1.53	1.50	1.47	1.43

TABLE II
Intensities

mode ν	cell thickness (cm)	conc. (mole/cc)	A_{gas} (cm^{-2})	Ramsay wing correction (percent)	$K''A_{\text{soln}}$ ($\text{cm}^{-2}\text{mm}^{-1}$) Equation (6) Ramsay	$K''A_{\text{soln}}$ ($\text{cm}^{-2}\text{mm}^{-1}$) +Figure 7 & 8 *Figure 9
ν_2	0.0162	$\sim 10^{-5}$	241^{13}	10.8 - 15.0	0.8 ± 0.1	0.8 ± 0.1
ν_3	0.0162	$\sim 10^{-5}$	2700^{19}	0, 0	3.0 ± 0.4 (non-Lorentzian)	4.2 ± 0.4
$\frac{(A_3/A_2)_{\text{soln}}}{(A_3/A_2)_{\text{gas}}}$	---	---	---	---	0.30	0.46† 0.44*

TABLE III
Solution to Gas Ratios

mode ν	Polo-Wilson Equation (20)	Person Equation (21)	Kalman-Decius Equation (22) (spherical)	Kalman-Decius Equation (24) (ellipsoidal)
ν_3	1.32	1.01	1.06	0.86
ν_2	1.32	1.01	1.12	1.41
$\frac{(A_{\text{soln}}/A_{\text{gas}})_3}{(A_{\text{soln}}/A_{\text{gas}})_2}$	1.00	1.00	1.06	0.60

TABLE IV
Band Centers and Shifts

mode ν	gas phase (cm^{-1})	solution phase (cm^{-1})	$\Delta\nu$ (cm^{-1})	$\Delta\nu_2/\Delta\nu_3$ experimental	$\Delta\nu_2/\Delta\nu_3$ theoretical (Equation 44)	$\Delta\nu_2/\Delta\nu_3$ theoretical (Equation 45)	X_{23} (cm^{-1}) gas	X_{23} (cm^{-1}) solution
ν_2	667 ¹³	658.5	8.5				--	--
ν_3	2350 ¹⁹	2336	14	0.61	0.16	0.33	--	--
$\nu_{3_{\text{hot}}}$	--	2325	--	--	--	--	-11.0 ⁶	-11

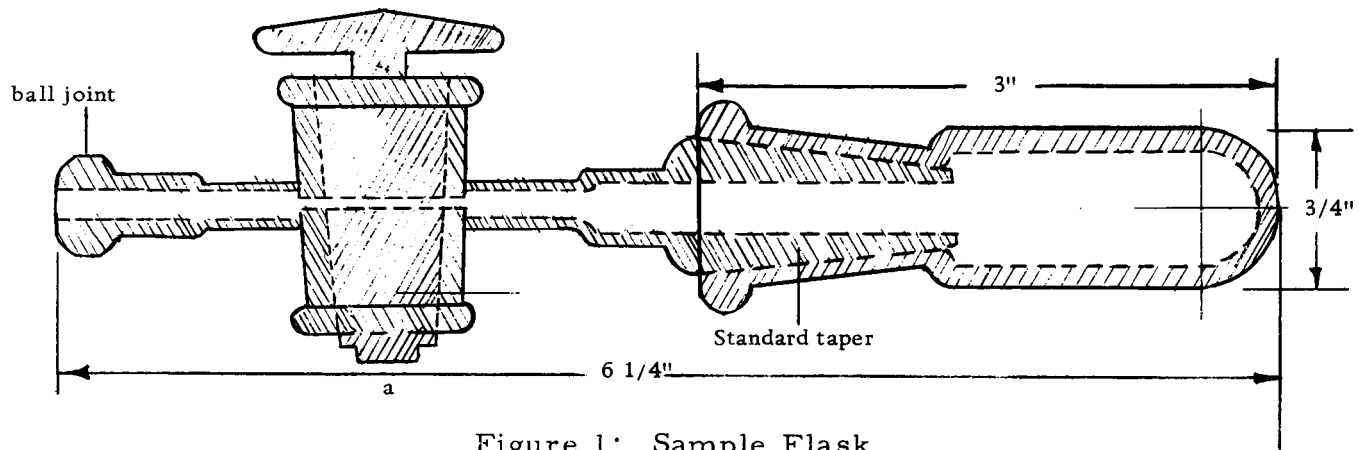


Figure 1: Sample Flask

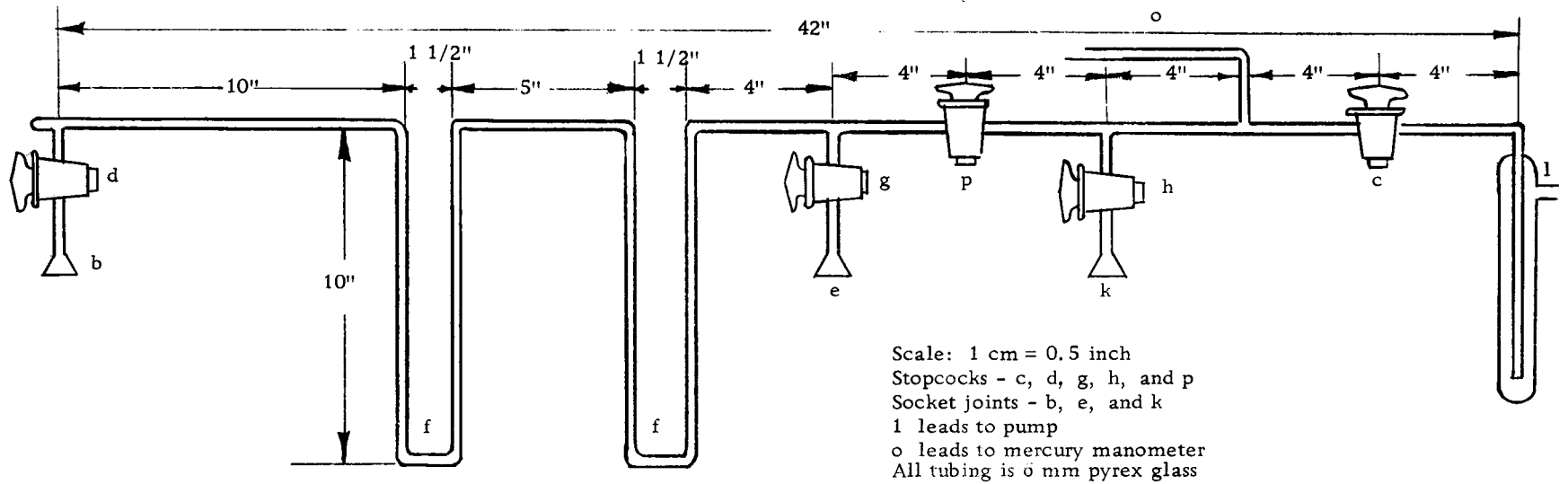
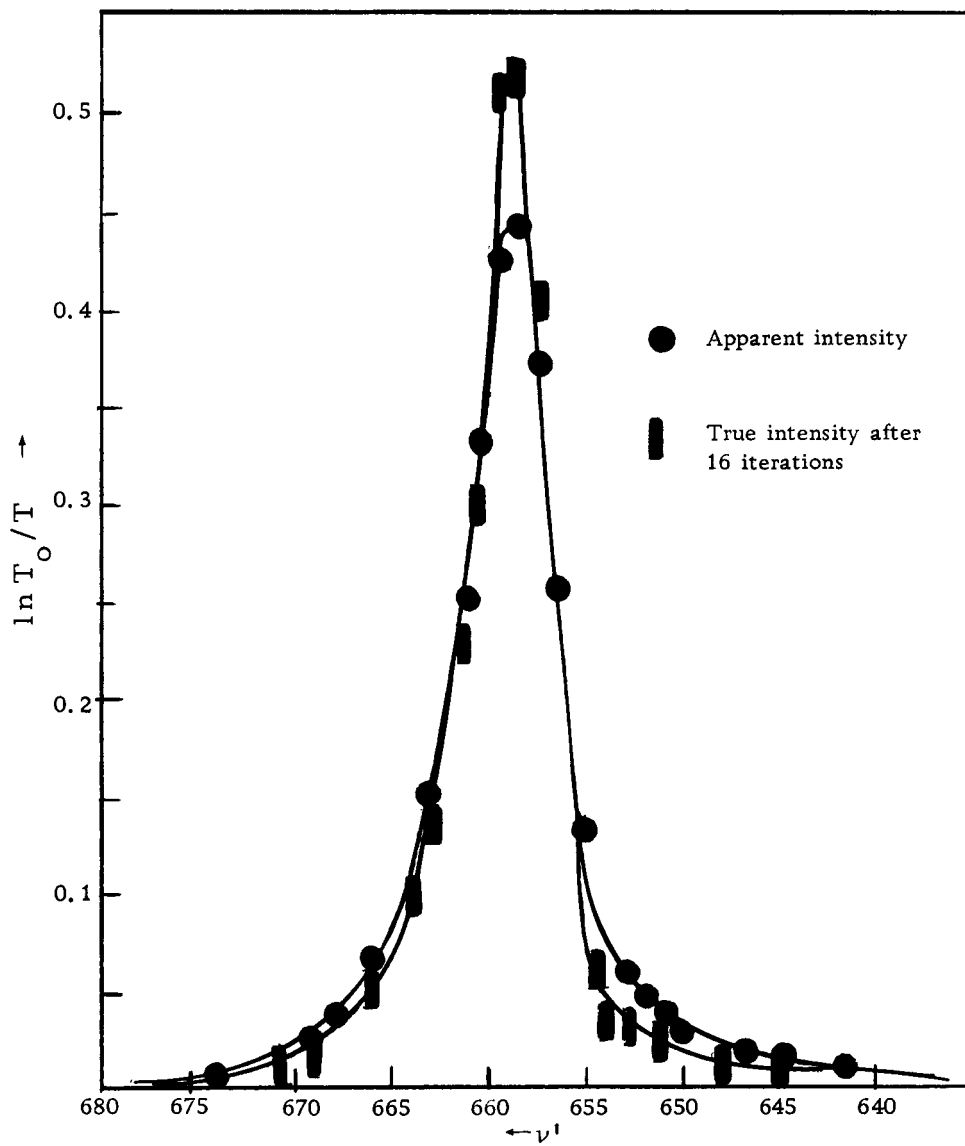


Figure 2: Vacuum Line

Figure 3: ν_2 mode

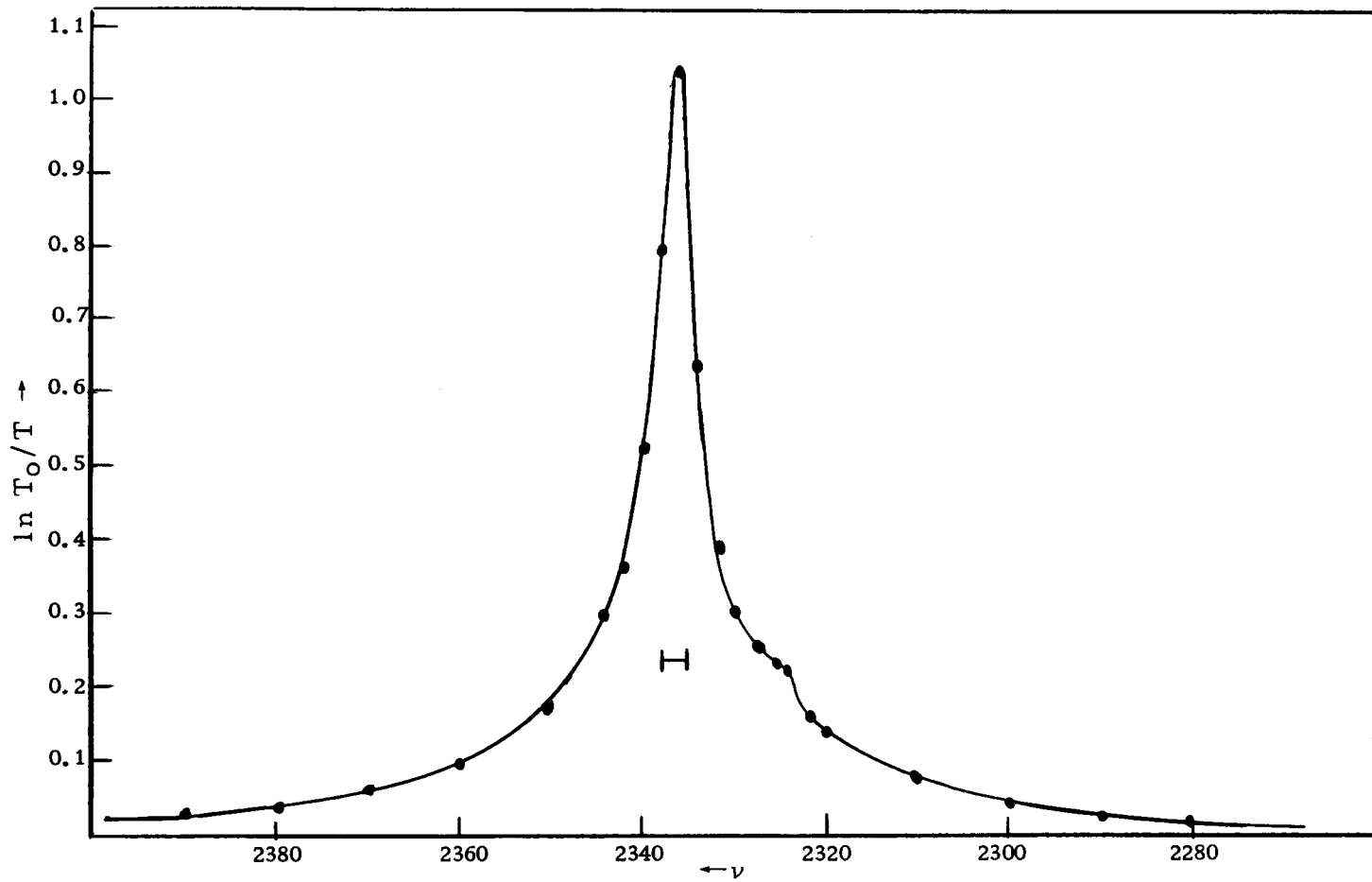


Figure 4: ν_3 mode

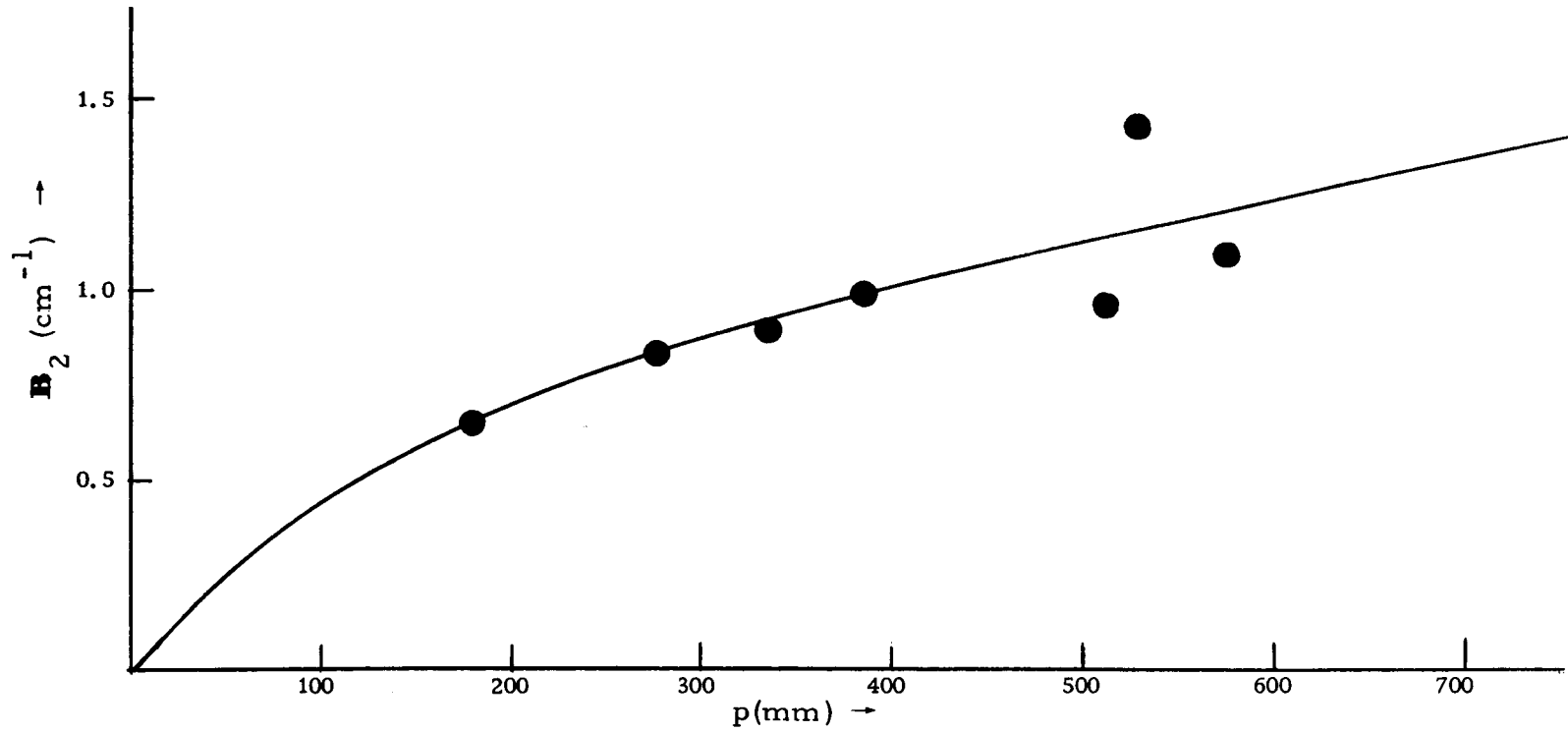


Figure 5: Plot of absorption area versus partial pressure of CO_2 for the ν_2 mode.

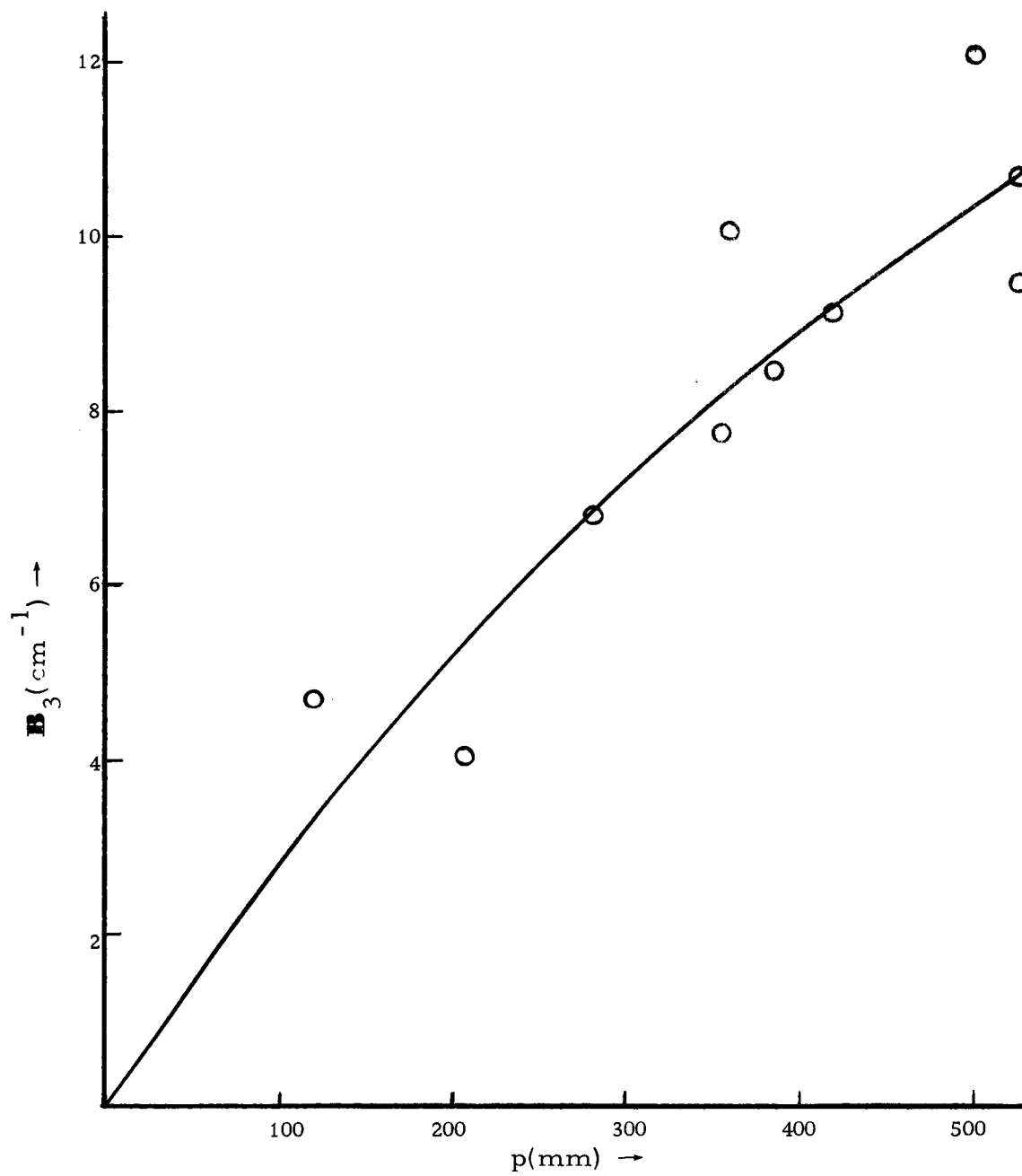


Figure 6: Plot of absorption area versus partial pressure of CO_2 for the ν_3 mode.

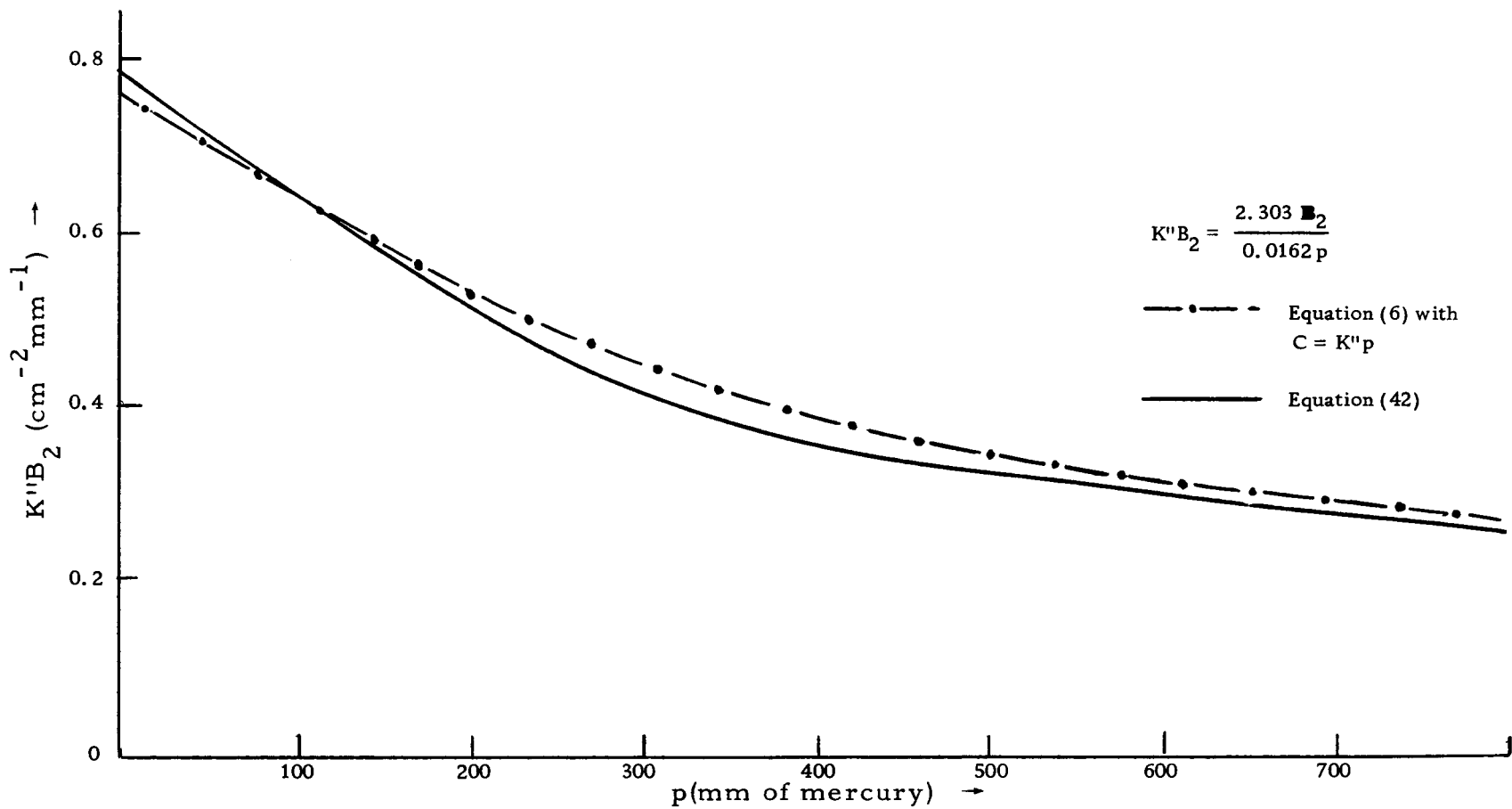


Figure 7: Plot of $K''B_2$ versus partial pressure of CO_2 for the ν_2 mode.

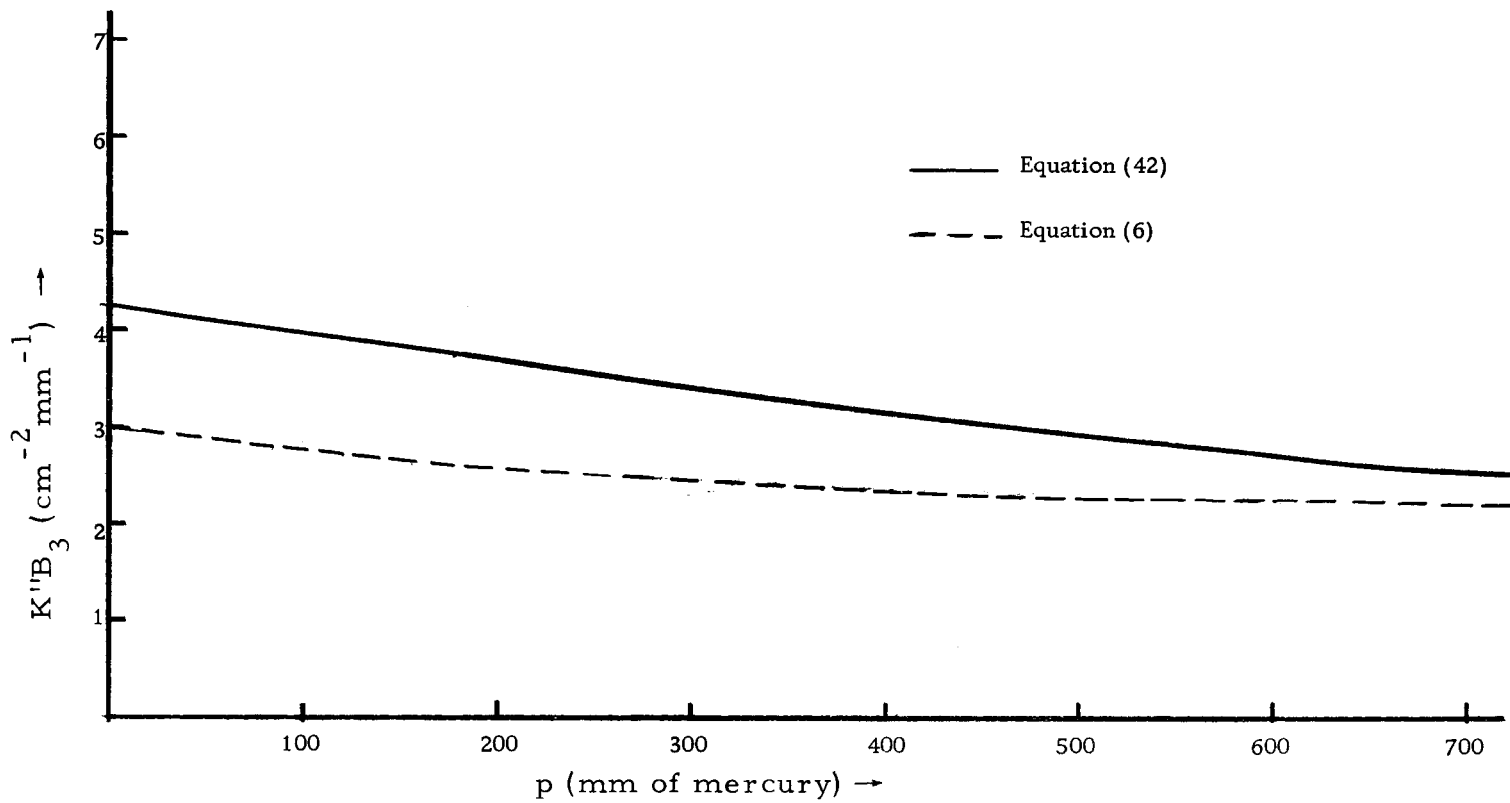


Figure 8: Plot of $K''B_3$ versus partial pressure of CO_2 for the ν_3 mode.

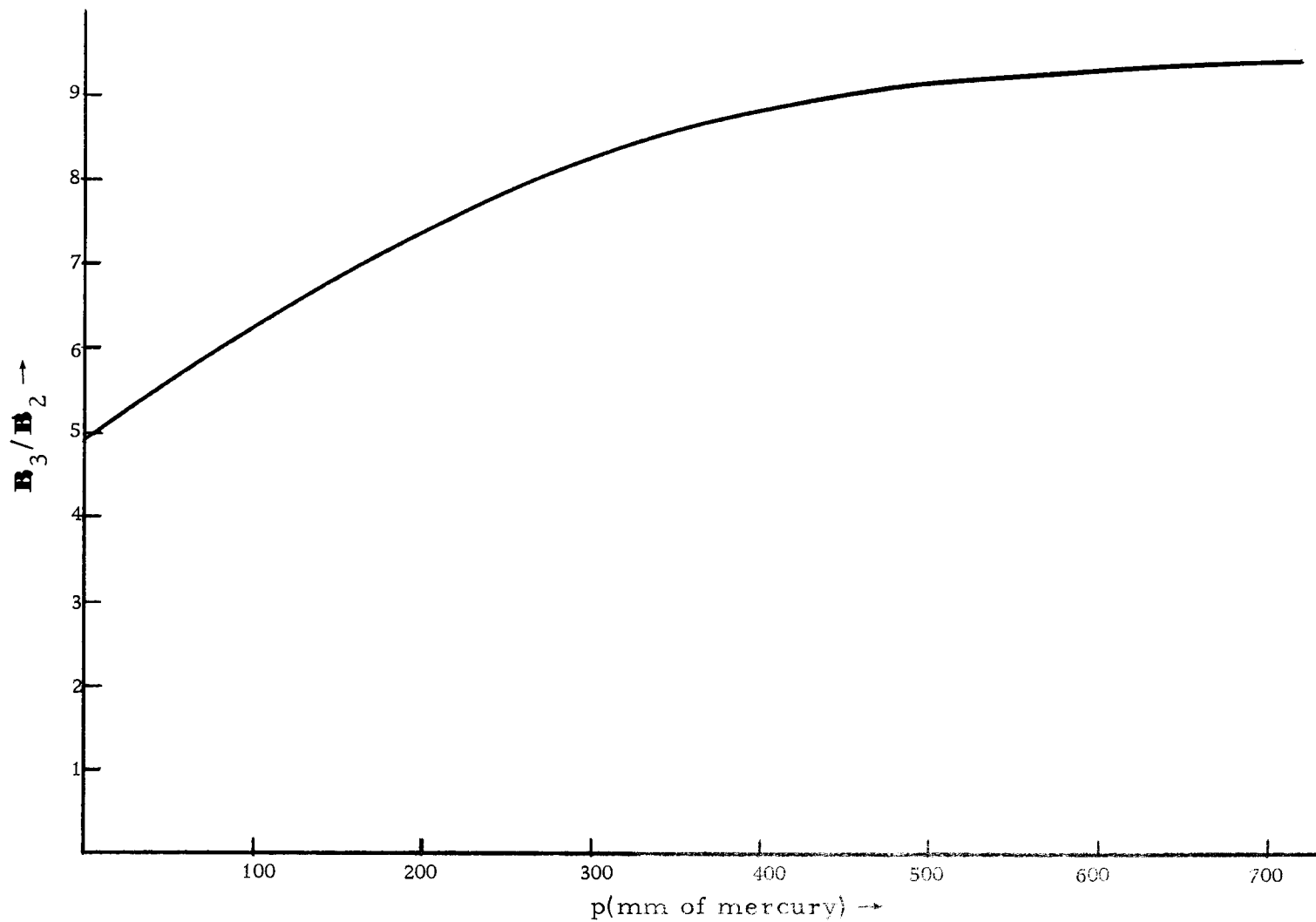


Figure 9. Plot of B_3/B_2 versus partial pressure of CO_2

BIBLIOGRAPHY

1. Barrow, G. M. Introduction to molecular spectroscopy. New York, McGraw-Hill Book Company, Inc., 1962. 318 p.
2. Barrow, G. M. Physical chemistry. New York, McGraw-Hill Book Company, Inc., 1961. 694 p.
3. Beckman Instruments, Inc. IR-7 infrared spectrophotometer instruction manual. Fullerton, California, 1960. 85 p.
4. Böttcher, C. J. F. Theory of electric polarisation. Amsterdam, Elsevier Publishing Company, 1952. 492 p.
5. Buckingham A. D. A theory of frequency, intensity, and band width changes due to solvents in infrared spectroscopy. Proceedings of the Royal Society of London 255A:32-39. 1960.
6. Herzberg, Gerhard. Infrared and Raman spectra. New York, Van Nostrand, 1954. 632 p.
7. International Union of Pure and Applied Chemistry Commission on Molecular Structure and Spectroscopy. Table of wave-numbers for calibration of infra-red spectrophotometers. Washington, Butterworths, 1961. p. 537-699.
8. Kalman, O. F. and J. C. Decius. Absolute infrared intensities of the CS_2 fundamentals in CCl_4 solution and of the 768-797 cm^{-1} Fermi Doublet of CCl_4 in Cyclohexane solution. Journal of Chemical Physics 35:1919-1924. 1961.
9. Khidir, A. L. and J. C. Decius. Numerical methods for the correction of apparent band shapes due to finite slit width. Spectrochimica Acta 18:1629-1639. 1962.
10. Maki, Arthur and J. C. Decius. Vibrational spectrum of cyanate ion in various alkali halide lattices. Journal of Chemical Physics 31:772-880. 1959.
11. National Research Council of the USA. International critical tables of numerical data, physics, chemistry, and technology. Vol. 2. New York, McGraw-Hill Book Company, Inc., 1927. 561 p.

12. Onsager, Lars. Electric moments of molecules in liquids. *Journal of the American Chemical Society* 58:1486-1493. 1936.
13. Overend, John, M. J. Youngquist, E. C. Curtis, and Bryce Crawford, Jr. Vibrational intensities XI. CO₂ and Wilson-Wells method. *Journal of Chemical Physics* 30:532. 1959.
14. Pauling, Linus and E. B. Wilson, Jr. Introduction to quantum mechanics. New York, McGraw-Hill Book Company, Inc., 1935. 468p.
15. Person, W. B. Liquid-gas infrared intensities, pressure induced absorption and the temperature dependence of infrared intensities in liquids. *Journal of Chemical Physics* 28:319-322. 1958.
16. Polo, S. R. and M. K. Wilson. Infrared intensities in liquid and gas phase. *Journal of Chemical Physics* 23:2376-2377. 1955.
17. Ramsay, D. A. Intensities and shapes of infrared absorption bands of substances in liquid phase. *Journal of the American Chemical Society* 74:7280. 1952.
18. Thorndike, A. M., A. J. Wells, and E. B. Wilson, Jr. The experimental determination of the intensities of infrared absorption bands. II. Measurement of ethylene and nitrous oxide. *Journal of Chemical Physics* 15:157-165. 1947.
19. Weber, D., R. J. Holm, and S. S. Penner. Integrated absorption vibrational rotational bands of CO₂. *Journal of Chemical Physics* 20:1820. 1952.
20. Wilson, E. B. Jr., J. C. Decius, and P. C. Cross. Molecular vibrations, the theory of infrared and Raman vibrational spectra. New York, McGraw-Hill Book Company, Inc., 1955. 388p.
21. Wilson, E. B. Jr. and A. J. Wells. The experimental determination of the intensities of infra-red absorption bands. *Journal of Chemical Physics* 14:578-580. 1946.
22. Yamaka, Haruka and Willis B. Person. Absolute infrared intensities of the fundamental absorption bands in solid CS₂. *Journal of Chemical Physics* 40:309-321. 1964.

APPENDIX

APPENDIX

Slit Function

Khidir and Decius (9) chose a triangular distribution for their slit function. Originating at the wing of the band, the $T:T_0$ ratios are separated by equal intervals of $\Delta\nu$. The spectral slit width, s , was then expressed in units of $\Delta\nu$. For simplicity s can take on only integer values. The coefficients in Equation (12) then become

$$a_0 = s/s^2$$

and
$$a_j = (s - j)/s^2; \quad j = 1, 2, 3, \dots, N - 1$$

Program Instructions for an Alwac IIIE, N = 64 (9)

Read program into computer through high speed reader. For a check on program call 44, 45, 50, 51, 52, and 53. Type 5000.

Read data through high speed reader. First read slit vector in the following form: e. g., for $s = 9 \text{ cm}^{-1}$, $\Delta\nu = 3 \text{ cm}^{-1}$, then $s = 3\Delta\nu$, or

.1111 .2222 .3333 .2222 .1111 .0 0 32 words

.1111 .2222 .3333 .2222 .1111 0 0 32 words

Next read into computer T/T_0 values, 64 of these. Reread the 29th, 30th, 31st, and 32nd as the 33rd, 34th, 35th, and 36th word.

To check input data type 5200. If T/T_0 , $\ln(T_0/T)$, and the integrated intensity are desired, then put jump switch one and two up. However, to skip a type out of T_0/T , put jump switch one down and two up.

Type 5100 to start computations. Iterate with jump switch one down and two up. After each iteration there will be a type out of the total number of iterations to date. For an output on next iteration put jump switch one and two up and push the P-N-S switch to start. This will give I/I_0 and integrated intensity. Should $\ln(I_0/I)$ also be desired along with I/I_0 and the integrated intensity, then push jump switch one down instead of up.

To check for convergence (i. e., $i_n - i_{n-1} \leq 0.05$ percent), put jump switch one and two up and push P-N-S to proceed, and the machine will output integrated intensity only.

The machine always halts on an output. To recycle, type 5100.

Note: With each new set of data type 5304 lb 11880000 for correct type out of the number of iterations accomplished.